Photochemical & Photobiological Sciences
https://doi.org/10.1007/s43630-022-00203-5

ORIGINAL PAPERS

Photoredox catalysis powered by triplet fusion upconversion: arylation of heteroarenes

Jorge Castellanos-Soriano[1] · Daniel Álvarez-Gutiérrez[1] · M. Consuelo Jiménez[1] · Raúl Pérez-Ruiz[1]

Received: 27 January 2022 / Accepted: 3 March 2022

Abstract

In this work, the feasibility of triplet fusion upconversion (**TFU**, also named triplet–triplet annihilation upconversion) technology for the functionalization (arylation) of furans and thiophenes has been successfully proven. Activation of aryl halides by **TFU** leads to generation of aryl radical intermediates; trapping of the latter by the corresponding heteroarenes, which act as nucleophiles, affords the final coupling products. Advantages of this photoredox catalytic method include the use of very mild conditions (visible light, standard conditions), employment of commercially available reactants and low-loading metal-free photocatalysts, absence of any sacrificial agent (additive) in the medium and short irradiation times. The involvement of the high energetic delayed fluorescence in the reaction mechanism has been evidenced by quenching studies, whereas the two-photon nature of this photoredox arylation of furans and thiophenes has been manifested by the dependence on the energy source power. Finally, the scaling-up conditions have been gratifyingly afforded by a continuous-flow device.

Graphical abstract

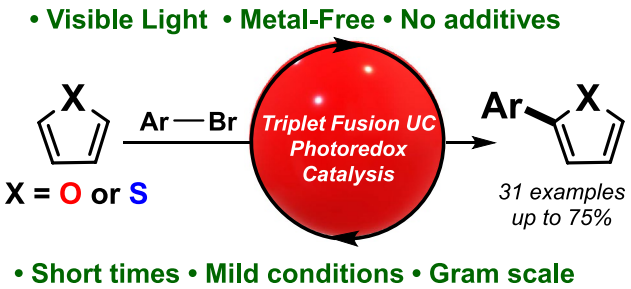

Keywords Visible light · Photoredox catalysis · Arylations · Furans · Thiophenes · Photon upconversion · Triplet fusion (triplet–triplet annihilation)

1 Introduction

Application of photon upconversion (UC) that transforms low-energy (visible light) into higher energy (UV or near-Vis) radiation has been potentially ranged from energy to biology fields constituting nowadays an active area of research [1–3]. The UC mechanism implies two types of scenarios, named two-photon absorption (TPA) [4] and triplet fusion upconversion (**TFU**, also so-called triplet–triplet annihilation, TTA) [5–7]. The latter proceeds with lower energetic radiation than TPA, and constitutes one of the most attractive wavelength conversion technologies, successfully applied in several scientific topics [8–18]. Thus, **TFU** involves the association of multistep photochemical events (Fig. 1B), and a variety of organic dyes and metal complexes can be currently found in literature for this purpose [19]. Briefly, after absorption of low energy photons ($h\nu_1$), the singlet excited state $^1S^*$ of the sensitizer (donor) is reached; then, intersystem crossing (ISC) leads to the corresponding triplet excited state $^3S^*$. Afterwards, intermolecular

✉ Raúl Pérez-Ruiz
raupreru@qim.upv.es

[1] Departamento de Química, Universitat Politècnica de València, Camino de Vera s/n, 46022 Valencia, Spain

Published online: 18 March 2022

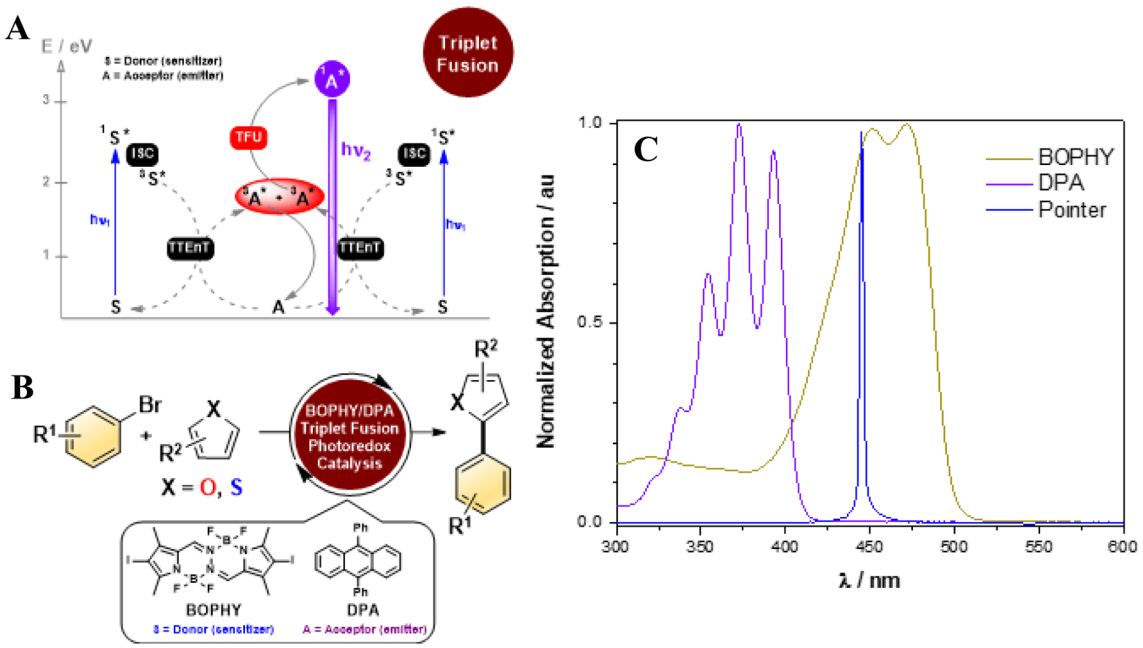

Fig. 1 **A** Application of **TFU** to the C–C coupling catalytic reaction between aryl bromides and furans or thiophenes using an appropriate donor/acceptor system as photocatalyst. **B** Photochemical events associated with the **TFU** technology. Energy-level diagram representing the photophysical and photochemical processes of a donor–acceptor system. **C** Normalized absorption spectra of **BOPHY** dye and **DPA** in acetonitrile/dimethylacetamide mixture. The blue line corresponds to the emission of the blue laser pointer

triplet–triplet energy transfer (TTEnT) from ^{3}S* to the emitter (acceptor, A) takes place, affording ^{3}A*. Finally, collision of two ^{3}A* units gives rise to the highly energetic ^{1}A*, which is capable to radiate anti-Stokes delayed fluorescence ($h\nu_2$).

In this context, visible-light photoredox catalysis represents a novel emerging strategy to drive chemical reactions [20–27]. Activation of molecules by visible light offers the possibility of new reaction routes, otherwise impossible to occur using classical nonphotochemical strategies. Frequently, photocatalytic processes require the employment of activated substrates that facilitate generation of radical intermediates in the vicinity of heteroatomic functional groups (amines, carbonyls) [28–30], or by irreversible reaction steps [31–34]. Consequently, photocatalytic activations of unbiased or non-activated substrates have received very little attention. In general, the scope of photocatalytic bond activations is limited not only by the low energy of photons laying in the visible range, only sufficient for the cleavage of weak C–I, Csp_3–Br and π-bonds, but also by the energetic losses suffered by the photocatalysts, such as intramolecular charge transfers or internal conversions [35–37].

Among other strategies such as consecutive photoinduced electron transfer or electrophotochemistry [38, 39], a novel possibility to overcome this limitation is the implementation of **TFU**. In the former methodologies, after exciting the photocatalyst (or reducing by electrode), reductive quenching of its excited state from sacrificial donor (or electrode) generates the reduced species that can become subsequently excited, producing an even more potent reductant. They differ from the **TFU** technology which provides high energy excited state from low energy light in a redox–neutral strategy. Despite the fact that this biphotonic process could be a useful synthetic tool in organic synthesis, only few examples are reported in the literature [40–48]. Thus, we wish to report the successful use of **TFU** photocatalysis for the challenge of heteroarene functionalization, a straightforward methodology that can be employed for the synthesis of natural products, bioactive compounds, and high value fine chemicals [49]. We have recently explored the feasibility of employing the **TFU** technology for the photocatalyzed arylation of *N*-methylpyrrole [45].

Herein, we focus our attention on the application of **TFU** to the C–C coupling between aryl bromides and furans or thiophenes (Fig. 1B). Similar photoreactions have been reported in the past employing metal-based or metal-free photoredox catalysts [50–57]; however, these methods present some drawbacks, such as the need of expensive and toxic noble-metal complexes as photocatalysts, the use of high activated starting materials (aryl iodides or aryl diazonium salts) that limits the accessible substrate scope, the presence of additives in the medium increasing the complexity of the system or the prolonged irradiation times (more than 10 h) implying unwanted processes. In this context,

TFU photoredox catalysis would offer some advantages over other photocatalytic-based protocols which include very mild reaction conditions (visible light, room temperature, atmospheric pressure), employment of stable and less activated commercially available reagents, absence of metal photocatalysts or other additives (sacrificial donors/acceptors) in the medium, and short irradiation times.

2 Results and discussion

2.1 Optimizing conditions for coupling reaction catalyzed by TFU

We focused on the arylation of furans and thiophenes using bis(difluoroboron)-1,2-bis((1H-pyrrol-2-yl)-methylene) hydrazine (**BOPHY**) as sensitizer and 9,10-diphenylanthracene (**DPA**) as emitter as photocatalytic system on the basis of literature data (Fig. 1C) [45]. For searching the optimal conditions, we initiated the investigation using 4-bromoacetophenone (**1a**) and furan (**2a**) as starting materials in the presence of catalytic amounts of **BOPHY/DPA** and the mixture was submitted to visible light irradiation through quartz with a commercially available blue laser pointer (λ_{exc} = 450 nm ± 10, 2 W, see Figure S1 in the Supporting Information). The desired coupled product **3a** was thus obtained after 2 h of irradiation using acetonitrile (ACN) as solvent (Table 1, entries 1–3); however, conversions and yields were low-to-moderate even using higher equivalents of **2a** (Table 1, entry 3). Conversely, full conversion of **1a** was detected in dimethylacetamide (DMA), although 42% yield of **3a** was gained together with significant amounts of acetophenone (**3a'**) as photo-reduced by-product (Table 1, entry 4). To reach the best conditions for conversion, product distribution and coupling product yield, we then performed the reactions using ACN/DMA mixtures (Table 1, entries 5–8). In a first attempt the results did not improve using an excess of DMA (Table 1, entry 5). Interestingly, when the ACN/DMA ratio was 3/1 v/v, good conversion was observed, yielding 51% of product **3a** (Table 1, entry 6). To gain better conversion/selectivity (DMA is a good H donor) the solvent ratio was modified to 4/1 v/v (Table 1, entries 7–11).

The optimized reaction conditions led to almost total conversion and 70% yield of **3a** after 2 h irradiation of **1a** (1 eq) and **2a** (100 eq) in the presence of catalytic amounts of **BOPHY** (1% mol) plus **DPA** (10% mol) in N_2-bubbled ACN/DMA mixture (Table 1, entry 9). As expected, formation of **3a** did not take place in the absence of **BOPHY** or **DPA** (Table 1, entries 10–11), confirming the key role of the **TFU** system in the investigated reaction. To mention that the excess of nucleophile (furan) was easily recovered by conventional chromatographic techniques. Besides, the reaction was also carried out using 4-iodoacetophenone as starting material, obtaining a 25% yield of the coupled product **3a** which was found to be clearly lower than that obtained with

Table 1 Searching the optimal conditions.[a]

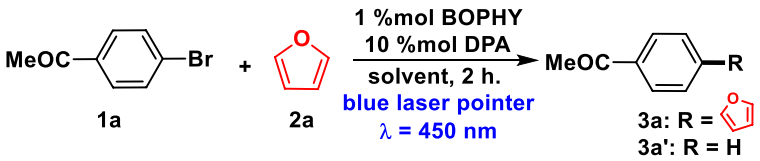

No	Solvent	**2a**/eq	Conv/%[b]	**3a**/**3a′**	Yield/%[b]
1	ACN	10	30	67/33	20
2	ACN	30	30	86/14	26
3	ACN	80	59	96/4	57
4	DMA	80	100	42/58	42
5	ACN/DMA (1/3)	80	74	54/46	40
6	ACN/DMA (3/1)	80	66	77/23	51
7	ACN/DMA (4/1)	80	81	79/21	64
8[c]	ACN/DMA (4/1)	80	87	73/27	64
9	**ACN/DMA (4/1)**	**100**	**90**	**78/22**	**70**[d]
10[e]	ACN/DMA (4/1)	100	0	0/0	0
11[f]	ACN/DMA (4/1)	100	0	0/0	0

[a][**1a**] = 10 mM (1 eq), [**2a**] as indicated, [**BOPHY**] = 0.1 mM (0.01 eq) and [**DPA**] = 1 mM (0.1 eq) in 3 mL of N2/solvent at 20 ºC; irradiation (blue laser pointer λ_{exc} = 450 nm ± 10, 2 W); [b]Conversion related to **1a**, GC-FID analysis vs. internal 1-dodecanenitrile. Mass balance was 100% in all cases otherwise indicated; [c]4 h of irradiation; [d]53% isolated yield; [e]without **BOPHY**; [f]without **DPA**.

the optimal reaction. A plausible explanation for this result could be the formation of iodide (heavy atom) in the medium that is a well-known singlet excited quencher and consequently provoking loss of efficiency of the **TFU** system.

2.2 Substrate scope

After standardizing the conditions, we studied the generality and applicability of this methodology to aryl bromides with different furan derivatives, where very good conversions and selectivities were in general obtained (Fig. 2). Hence, arylation of **2a** was also achieved satisfactorily in the presence of 4-bromobenzaldehyde (**1b**) and 4-bromobenzonitrile (**1c**) as starting reagents, obtaining the desired products (**3b**–**c**). The reaction was tolerant in terms of regioselectivity, since 2-bromoaryl compounds could also functionalize different furans (**3d**–**f**, **3m–n**). Reaction proceeded efficiently using **1a** or **1c** and several 2-substituted furans bearing different substituents, such as nitrile (–CN), ester (–COOMe), carbonyl (COMe) groups or alkylated chains, affording the corresponding coupling products (**3g**–**l**). Formation of **3c** (60% yield) was comparable to that from example of donor–acceptor-type organic photocatalyst (46%) [52], despite of the shorten irradiation time and the absence of additives. Finally, hetero bicyclic compounds such as quinoline could also be coupled to furan (**3o**–**p**), giving rise to regioisomers.

The arylation of thiophenes was also photocatalyzed by **BOPHY/DPA** system using visible light as energy source. The outputs in terms of conversion and selectivities were found to be in a lesser extent than those for furans (Fig. 2). Two main reasons could explain that the reactivity of thiophenes towards electrophilic substitution is less than furans: (1) the most aromatic character of the former and, (2) the *p*-electrons of the sulphur atom are in the *3p* orbital which overlaps less effectively than the *2p* orbital of oxygen with the *2p* orbitals of carbon. We decided to increase the equivalents of thiophene derivatives with the occurrence of directing the process towards the formation of the final product to adjust the reaction conditions at the optimal state. Remarkably, the production of such amount of arylated thiophenes (**5a**–**k**) evidenced the key role of the **TFU** couple as suitable photocatalyst system for such synthetic purpose. In line with furans, the method allowed the introduction of *ortho*- or *para*-substituted aryls to thiophenes, where the production of regioisomers was also feasible (**5l**–**l′** and **5m**–**n**).

2.3 Mechanistic proposal

The proposed reaction mechanism is outlined in Fig. 3. Following similar performance [45], the reaction then starts with the selective absorption of **BOPHY** dye at $\lambda_{irr} = 450$ nm. After ISC from the singlet to the triplet, a rapid TTEnT occurs to produce quantitatively ^{3}**DPA*** which collides with another ^{3}**DPA*** to generate the ^{1}**DPA*** upconverted fluorescence. A single electron transfer (SET) from ^{1}**DPA*** to the aryl bromide (Ar–Br) leads to the radical ion pair, Ar–Br$^{\bullet-}$ and **DPA**$^{\bullet+}$. Fast scission of the Ar–Br$^{\bullet-}$ gives rise to bromide (Br$^-$) plus the aryl radical (Ar$^\bullet$) that is successfully trapped by the 5-membered heteroarene, affording

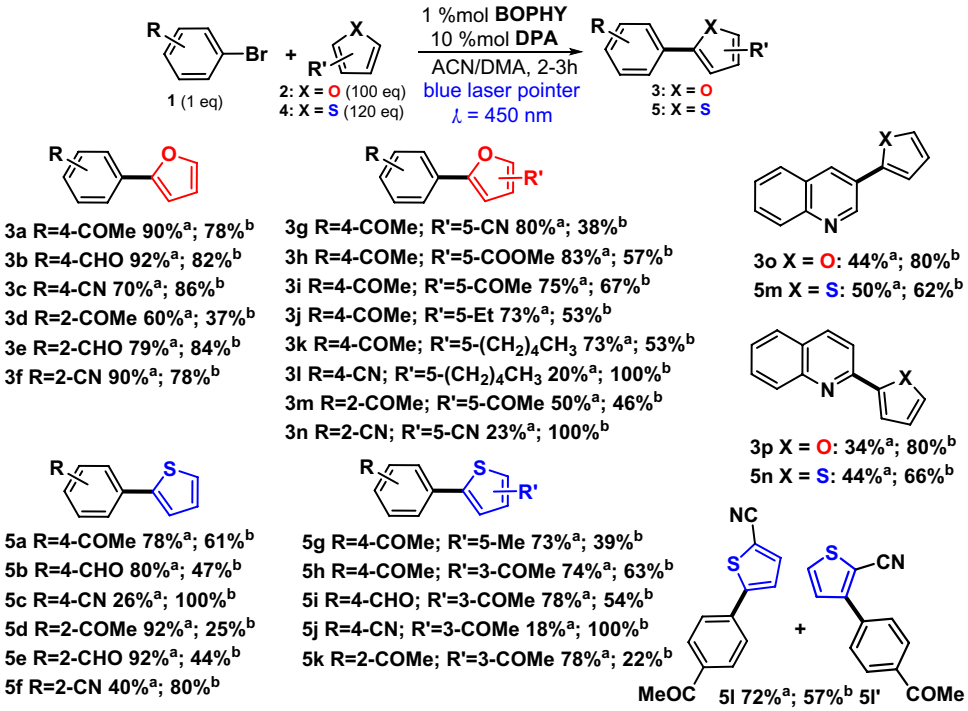

Fig. 2 Substrate scope for the arylation of furans and thiophenes using **TFU** as photocatalyst system. Mass balance was 100% in all cases. [a]Conversion related to **1**; [b]selectivity

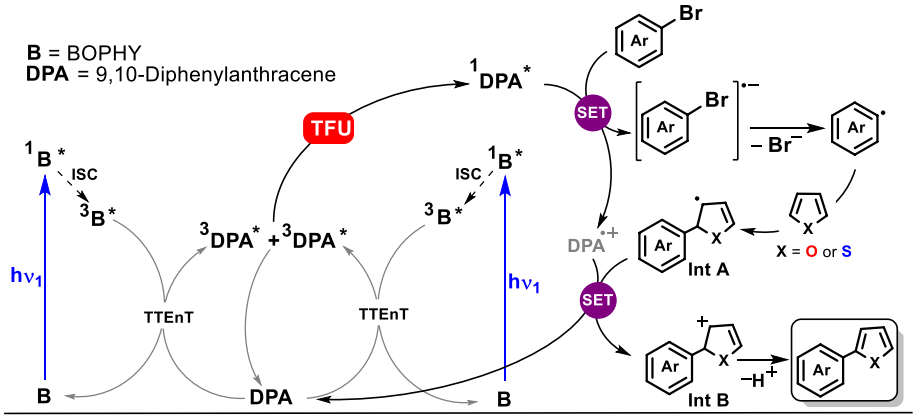

Fig. 3 Proposed reaction mechanism for the photocatalytic arylation of furans or thiophenes by means of **TFU** technology

the radical intermediate **A** (Int **A**). A SET from Int **A** to **DPA**$^{\cdot+}$ provides the restoring of **DPA** and the cationic intermediate **B** (Int **B**) which evolves to the final product after deprotonation.

The involvement of the high-energy delayed fluorescence ^{1}**DPA*** in the SET was supported by quenching experiments (Fig. 4A; Figures S2–S3). Clearly, a decrease of ^{1}**DPA*** was observed in the presence of increasing amounts of quenchers, confirming the interaction between ^{1}**DPA*** and the aryl bromides. The quenching rate constants (k_q) were calculated by the Stern–Volmer analysis (Fig. 4B; Equations S1 and S2). The Stern–Volmer constants (K_{SV}) were thus estimated as 44, 79 and 18 M^{-1} for **1a**, **1b** and **1c**, respectively. From these data and the **DPA** singlet lifetime value ($\tau_F = 6.96$ ns in aerated ACN(4)/DMA(1) solution at 0.01 mM, Figure S4), the $k_q(S_1)$ were found to be 6.3×10^9 M^{-1} s^{-1} (for **1a**), 1.1×10^{10} M^{-1} s^{-1} (for **1b**) and 2.6×10^9 M^{-1} s^{-1} (for **1c**). These results indicated that interaction of ^{1}**DPA*** with the aryl bromides occurred at diffusion rates. To worth mentioning that a good correlation might be established between starting material conversion in the steady-state irradiations and fluorescence quenching measurements.

Besides, the diversity in reactivity was directly linked to thermodynamic and kinetic data (see Table S1). The SET pathway was assumed to be the rate-determining step, considering that fragmentation of Ar–Br$^{\cdot-}$ and trapping of Ar$^{\cdot}$ by the large excess of the heteroarenes were found to be very fast processes. Hence, the activation barriers of both SET vs. BET (Table S1) supported that the weak reactivity in some cases was in accordance with an efficient reversibility of the electron transfer process.

To verify the necessity of light to maintain the coupling, we investigated a "light/dark" experiment in the reaction of **1b** with **2a** in the presence of the **TFU** system under optimal conditions (Fig. 5A). It was observed that the reaction progressed steadily with visible light irradiation, but consumption of the aryl bromide abruptly stalled when the light source was removed. The results of this experiment did not definitively rule out a radical chain propagation mechanism

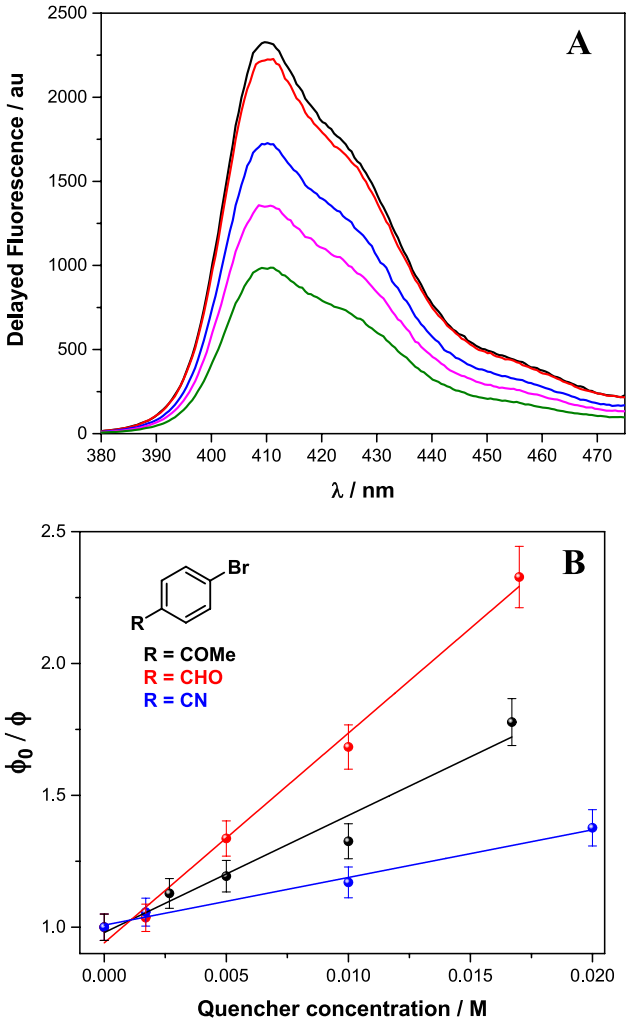

Fig. 4 **A** Delayed fluorescence spectra of a mixture of **BOPHY** (0.1 mM) and **DPA** (1 mM) in degassed ACN/DMA (4/1 v/v) recorded 1 μs after excitation with a pulsed laser ($\lambda_{exc} = 485$ nm) in the presence of increasing amounts of 4-bromobenzaldehyde **1b** (0 mM black, 1.7 mM red, 5 mM blue, 10 mM magenta and 17 mM green). **B** Stern–Volmer plots to obtain k_q (S_1); experimental errors were lower than 5% of the obtained values

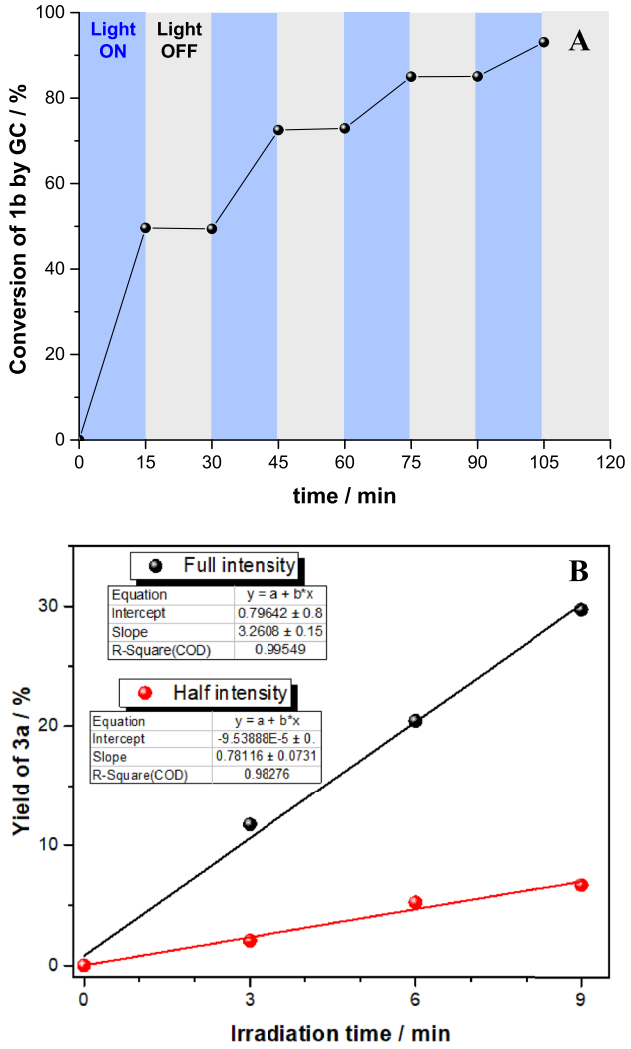

Fig. 5 **A** Light/dark experiment of the photoredox catalysed coupling reaction between **1b** and **2a** in the presence of **TFU** system as photocatalyst. **B** Two reactions with the same amount of **1a** (1 eq), **2a** (100 eq), **BOPHY** (1% mol), **DPA** (10% mol) in ACN/DMA (4/1 v/v) under nitrogen atmosphere were irradiated with the same blue laser pointer. Formation of **3a** was determined by GC analysis

by SET from Int **A** to the aryl bromide, although it was evident that visible light was a necessary component of the reaction. Furthermore, similar photoreactivity using pyrroles as trapping nucleophile showed that the possibility of a radical chain propagation appeared to be thermodynamically unfeasible [58].

Finally, the biphotonic nature of this photoredox catalytic process at reaction conditions was demonstrated by its dependence on the light source power (Fig. 5B). Shorter irradiation time (9 min) was used to prevent other influencing factors such as adverse effects of prolonged reaction time. Yields were determined by GC analysis with 1-dodecanenitrile as internal standard. Thus, upon increasing the blue laser pointer power from half to full intensity, the rate of product generation was found to enhance by a factor of 4.1 (resulting from ratio of 3.2608 to 0.78116 from the slopes of the linear regression fits) which supported an overall two-photon mechanism [41, 59, 60]. To gain further insight into mechanistic aspects relying on biphotonic excitation, a non-linear power dependency of the product yield (determined by GC–FID analysis) should operate. Hence, the model reaction (Table 1, entry 9) was submitted to different laser pointer intensities and a non-linear behavior was observed (Figure S5). Biphotonic reactions, therefore, proceed with high photon fluxes (higher yields are observed) which, in principle, might entail an increment of the likelihood for the catalytic system photodegradation. In this context, the utilization of this **TFU** system appeared to be advantageous, since negligible degradation of DPA was detected after irradiation (see for instance Figures S6–S7).

2.4 Scaling-up

The scalability of photochemical transformations by simply enlarging the reaction vessel (quite typical in thermal reactions in the laboratory) does not appear to be an efficient method; this could be explained by the attenuation of light penetration. To address this drawback continuous-flow photochemical devices have been developed for the scale-up of several processes [61–64]. Encouraged by the idea that **TFU** photoredox catalysis could be successfully applied to gram scale, we carried out the coupling reaction between **1a** (or **1b**) with **2a** in the presence of the **TFU** system under flow settings (Fig. 6). In a glass bottle, the reaction mixture under anaerobic conditions was delivered to a quartz cuvette holder (constant temperature at 20 °C due to water cooling) by a Fisher® continuous-flow pump through a Tygon Pharmed® BPT tubing (ID 1.6 mm). The sample kept continuously stirring in the quartz cuvette to facilitate the flow at the irradiation region, where the blue laser pointer ($\lambda_{exc} = 445$ nm ± 10) acted as visible light source. Gratifyingly, not only the coupled products 3a and 3 h were obtained in hundreds of milligrams but also the selectivity of the process was found to be 100% (Figures S6, S7), representing, therefore, a useful method for organic synthesis.

3 Conclusions

In summary, we have demonstrated that arylation of furans or thiophenes by a C–C coupling reaction can be successfully achieved using a **TFU** bimolecular system as photocatalyst. The reaction displays a broad scope toward aryl halides and furans or thiophenes with an acceptable range of functional group tolerance. The potential of this strategy lies on the advantage of using substrates commercially available,

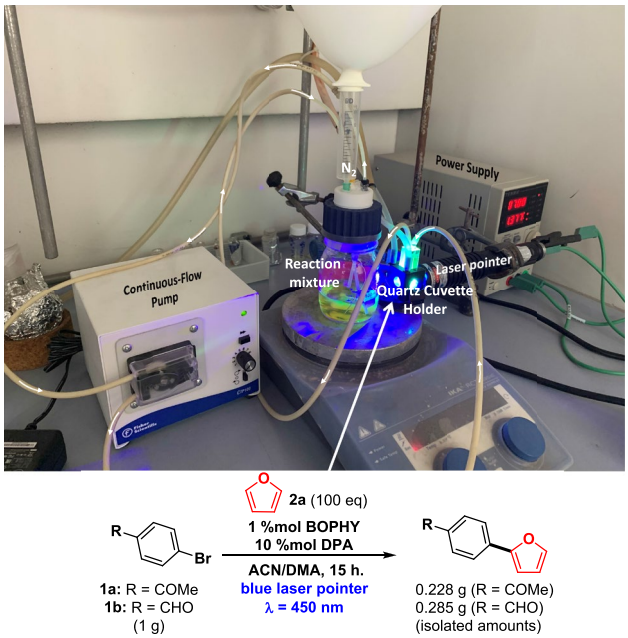

Fig. 6 Photograph of the setup of the home-made continuous-flow photochemical device for the gram-scale arylation of furan photocatalyzed by **TFU** technology

metal-free photocatalysts, no additives, visible light, and short reaction times. Mechanistic evidence has been demonstrated by laser flash photolysis, where the high energetic delayed fluorescence of **DPA** is directly implied on the activation of aryl halides. Finally, the biphotonic nature of this photoredox arylation of furans and thiophenes has been supported by the power dependence of the energy source. We believe that triplet fusion upconversion technology can be potentially applied in photoredox catalysis and further synthetic purposes employing this methodology beyond C–C coupling will be undertaken in the future.

4 Experimental

4.1 Materials and methods

All reagents (≥ 97% purity) and solvents (≥ 99% purity) were purchased from commercial suppliers (Merck, TCI, Apollo Scientific, Fluorochem, Scharlab) and used as received unless otherwise indicated. The dye BOPHY was synthesized as previously described (Ref. 10d in the main text), whereas the acceptor 9,10-diphenylanthracene (DPA) is commercially available. Reactions were carried out in a quartz cuvette (4 mL, Hellma) sealed with septum. Irradiation was performed using a blue diode laser pointer with a real power of 2000 mW ($\lambda_{exc} = 445\ nm \pm 10$, beam diameter of 10 mm) that was purchased from ®TorLaser. TLC was performed on commercial SiO_2-coated aluminium plates (DC60 F254, Merck). Visualization was done by UV-light (254 nm). 1-Dodecanenitrile was used as an internal standard in the GC quantitative measurements; yield products were estimated as: [conversion × selectivity]/mass balance. Determination of purity and structure confirmation of the literature known products was performed by ^{1}H NMR, ^{13}C NMR and low-resolution mass spectrometry (LRMS)–LRMS measurements were replaced by high-resolution mass spectrometry (HRMS) in case of unknown products. NMR spectral data were collected on a Bruker Advance 400 (400 MHz for ^{1}H; 101 MHz for ^{13}C) spectrometer at 20 °C. Chemical shifts are reported in δ/ppm, coupling constants J are given in Hertz. Solvent residual peaks were used as internal standard for all NMR measurements. The quantification of ^{1}H cores was obtained from integrations of appropriate resonance signals. Abbreviations used in NMR spectra: s—singlet, d—doublet, t—triplet, q—quartet, m—multiplet, bs—broad singlet, dd—doublet of doublet, ddd—doublet of doublet of doublet. HRMS was carried out was performed in the mass facility of SCSIE University of Valencia. LRMS was carried out on an HP 6890 Series GC System with Agilent 5973 Network Mass Selective Detector and H_2 as carrier gas. Abbreviations used in MS spectra: M—molar mass of target compound, EI—electron impact ionization, ESI—electrospray ionization.

4.2 General procedure for the arylation of furans or thiophenes

In a quartz cuvette (4 mL) with a magnetic stirring bar, an ACN (2.4 mL) + DMA (0.6 mL) solution of aryl halide (30 µmol, 0.01 M, 1.0 eq), **BOPHY** (100 µg, 0.3 µmol, 10^{-4} M, 0.01 eq), **DPA** (1 mg, 3 µmol, 10^{-3} M, 0.1 eq) and 1-dodecanenitrile (6.5 µL, 0.01 M, 1 eq) was prepared. The cuvette was sealed with a septum and placed in a water-cooling holder to keep a constant temperature around 20 °C (see Figure S1). The mixture was first purged with a nitrogen gas flux for 10 min, then furan (1 M, 100 eq) or thiophene (1.2 M, 120 eq) was added to the mixture which was subsequently maintained by nitrogen atmosphere during the photolysis. Then, 2 h irradiation of the reaction was performed with an external diode laser pointer ($\lambda_{exc} = 445\ nm \pm 10$) through one face of the cuvette. The reaction progress was monitored by GC–FID analysis. For isolation purposes, water (10 mL) was added, and the aqueous phase was extracted with ethyl acetate (3 × 10 mL). The combined organic phases were washed with brine (10 mL), dried over magnesium sulphate, filtered from the drying agent, and concentrated in vacuum. The crude product was purified by high-performance liquid chromatography (HPLC), using acetonitrile:water (80:20 v/v) as eluent.

4.3 Delayed emissions recorded by laser flash photolysis

The LP980–KS Laser Flash Photolysis Spectrometer (from Edinburgh Instruments) is a combined system for the measurement of laser induced transient absorption, emission kinetics and spectra, with the ability to automatically convert and fully analyze the kinetic and spectral information. The probe pulse is longer than the recorded time window of a measurement, and a monochromator (TMS302-A, grating 150 lines mm^{-1}) disperses the probe light after it passed the sample. The probe light can be then passed on to a PMT detector (spectral S5 range 200–870 nm) to obtain the temporal resolved picture. All components are controlled by the software L900 provided by Edinburgh.

For our delayed emission measurements, the probe shutter is closed so that no light from the Xe lamp is exciting the sample and the laser is only used as a light source. To photolyze our samples, a 485 nm monowavelength was employed, ensuring that only the **BOPHY** chromophore absorbs the excited photons. The data have been acquired as an average of several shots to improve the signal-to-noise ratio.

4.4 Fluorescence lifetime

Lifetime measurement of **DPA** (0.01 mM in aerated ACN/DMA 4/1 v/v) was carried out using an EasyLife X system containing a sample compartment composed of an automated Peltier cuvette holder to control the temperature, a pulsed LED excitation source and a lifetime detector. The employed LED excitation source was 372 nm, with emission filter of GG400.

4.5 Light/dark experiment

In a quartz cuvette (4 mL) with a magnetic stirring bar, an ACN (2.4 mL) + DMA (0.6 mL) solution of 4-bromobenzaldehyde **1b** (5.5 mg, 30 µmol, 0.01 M, 1.0 eq), BOPHY (100 µg, 0.3 µmol, 10^{-4} M, 0.01 eq), DPA (1 mg, 3 µmol, 10^{-3} M, 0.1 eq) and 1-dodecanenitrile (6.5 µL, 0.01 M, 1 eq) was prepared. The cuvette was sealed, placed in a water-cooling holder for keeping a constant temperature (20 °C). The mixture was first purged with nitrogen for 10 min, then furan **2a** (1 M, 100 eq) was added to the mixture. The reaction was alternatively irradiated with an external diode laser pointer and kept in the dark in 15-min intervals. Aliquots of 50 µL were removed at the start and after each interval and diluted with ACN. Conversion of the starting material was determined by GC–FID and based on 1-dodecanenitrile as internal standard.

Supplementary Information The online version contains supplementary material available at https://doi.org/10.1007/s43630-022-00203-5.

Acknowledgements We thank the Generalitat Valenciana (project CIDEGENT/2018/044) and the Spanish Government (project PID2019-105391GB-C22 funded by MCIN/AEI/10.13039/501100011033 and fellowship PRE2020–093783 funded by MCIN/AEI/10.13039/501100011033) for financial support. We also thank Prof. Julia Pérez-Prieto for spectroscopy facilities.

Funding Open Access funding provided thanks to the CRUE-CSIC agreement with Springer Nature.

Declarations

Conflict of interests The authors declare no competing financial interests.

References

1. Sun, Q.-C., Ding, Y. C., Sagar, D. M., & Nagpal, P. (2017). Photon upconversion towards applications in energy conversion and bioimaging. *Progress in Surface Science, 92*, 281–316. https://doi.org/10.1021/cm020897u
2. Frazer, L., Gallaher, J. K., & Schmidt, T. W. (2017). Optimizing the efficiency of solar photon upconversion. *ACS Energy Letters, 2*, 1346–1354. https://doi.org/10.1021/acsenergylett.7b00237
3. Gulzar, A., Xu, J., Yang, P. G., He, F., & Xu, L. (2017). Upconversion processes: Versatile biological applications and biosafety. *Nanoscale, 9*, 12248–12282. https://doi.org/10.1039/C7NR01836C
4. He, G. S., Tan, L.-S., Zheng, Q. D., & Prasad, P. N. (2008). Multiphoton absorbing materials: Molecular designs, characterizations, and applications. *Chemical Reviews, 108*, 1245–1330. https://doi.org/10.1021/cr050054x
5. Bharmoria, P., Bildirir, H., & Moth-Poulsen, K. (2020). Triplet-triplet annihilation based near infrared to visible molecular photon upconversion. *Chemical Society Reviews, 49*, 6529–6554. https://doi.org/10.1039/D0CS00257G
6. Rauch, M. P., & Knowles, R. R. (2018). Applications and prospects for triplet-triplet annihilation photon upconversion. *Chimia, 72*, 501–507. https://doi.org/10.2533/chimia.2018.501
7. Singh-Rachford, T. N., & Castellano, F. N. (2010). Photon upconversion based on sensitized triplet–triplet annihilation. *Coordination Chemistry Reviews, 254*, 2560–2573. https://doi.org/10.1016/j.ccr.2010.01.003
8. Barawi, M., Fresno, F., Pérez-Ruiz, R., & de la Peña O'Shea, V. A. (2019). Photoelectrochemical hydrogen evolution driven by visible-to-ultraviolet photon upconversion. *ACS Appl. Energy Mater., 2*, 207–211. https://doi.org/10.1021/acsaem.8b01916
9. Yanai, N., & Kimizuka, N. (2017). New triplet sensitization routes for photon upconversion: Thermally activated delayed

fluorescence molecules, inorganic nanocrystals, and singlet-to-triplet absorption. *Accounts of Chemical Research, 50*, 2487–2495. https://doi.org/10.1021/acs.accounts.7b00235
10. Schulze, T. F., & Schmidt, T. W. (2015). Photochemical upconversion: Present status and prospects for its application to solar energy conversion. *Energy Environ Science, 8*, 103–125. https://doi.org/10.1039/C4EE02481H
11. Zhou, J., Liu, Q., Feng, W., Sun, Y., & Li, F. (2015). Upconversion luminescent materials: Advances and applications. *Chemical Reviews, 115*, 395–465. https://doi.org/10.1021/cr400478f
12. Chen, G., Qiu, H., Prasad, P. N., & Chen, X. (2014). Upconversion nanoparticles: Design, nanochemistry, and applications in theranostics. *Chemical Reviews, 114*, 5161–5214. https://doi.org/10.1021/cr400425h
13. Castellano, F. N., & Schmidt, T. J. (2014). Photochemical upconversion: The primacy of kinetics. *Journal of Physical Chemistry Letters, 5*, 4062–4072. https://doi.org/10.1021/jz501799m
14. McCusker, C. E., & Castellano, F. N. (2013). Orange-to-blue and red-to-green photon upconversion with a broadband absorbing copper(I) MLCT sensitizer. *Chemical Communications, 49*, 3537–3539. https://doi.org/10.1039/C3CC40778K
15. Börjesson, K., Dzebo, D., Albinsson, B., & Moth-Poulsen, K. (2013). Photon upconversion facilitated molecular solar energy storage. *J. Mater. Chem. A*. https://doi.org/10.1039/C3TA12002C
16. Guo, S., Wu, W., Guo, H., & Zhao, J. (2012). Room-temperature long-lived triplet excited states of naphthalenediimides and their applications as organic triplet photosensitizers for photooxidation and triplet-triplet annihilation upconversions. *Journal of Organic Chemistry, 77*, 3933–3943. https://doi.org/10.1021/jo3003002
17. Gallavardin, T., Armagnat, C., Maury, O., Baldeck, P. L., Lindgren, M., Monnereau, C., & Andraud, C. (2012). An improved singlet oxygen sensitizer with two-photon absorption and emission in the biological transparency window as a result of ground state symmetry-breaking. *Chemical Communications, 48*, 1689–1691. https://doi.org/10.1039/C2CC15904J
18. Khnayzer, R. S., Blumhoff, J., Harrington, J. A., Haefele, A., Denga, F., & Castellano, F. N. (2012). Upconversion-powered photoelectrochemistry. *Chemical Communications, 48*, 209–211. https://doi.org/10.1039/C1CC16015J
19. Gertsen, A. S., Koerstz, M., & Mikkelsen, K. V. (2018). Benchmarking triplet-triplet annihilation photon upconversion schemes. *Physical Chemistry Chemical Physics, 20*, 12182–12192. https://doi.org/10.1039/C8CP00588E
20. Hossain, A., Bhattacharyya, A., & Reiser, O. (2019). Copper's rapid ascent in visible-light photoredox catalysis. *Science, 364*, 450. https://doi.org/10.1126/science.aav9713
21. Zhou, Q. Q., Zou, Y. Q., Lu, L. Q., & Xiao, W. J. (2019). Visible-light-induced organic photochemical reactions through energy-transfer pathways. *Angewandte Chemie International Edition, 58*, 1586–1604. https://doi.org/10.1002/anie.201803102
22. Strieth-Kalthoff, F., James, M. J., Teders, M., Pitzer, L., & Glorius, F. (2018). Energy transfer catalysis mediated by visible light: Principles, applications. *Chemical Society Reviews, 47*, 7190–7202. https://doi.org/10.1039/C8CS00054A
23. Twilton, J., Le, C., Zhang, P., Shaw, M. H., Evans, R. W., & MacMillan, D. W. C. (2017). The merger of transition metal and photocatalysis. *Nature Reviews Chemistry, 1*, 0052. https://doi.org/10.1038/s41570-017-0052
24. Romero, N. A., & Nicewicz, D. A. (2016). Organic photoredox catalysis. *Chemical Reviews, 116*, 10075–10166. https://doi.org/10.1021/acs.chemrev.6b00057
25. Skubi, K. L., Blum, T. R., & Yoon, T. P. (2016). Dual catalysis strategies in photochemical synthesis. *Chemical Reviews, 116*, 10035–10074. https://doi.org/10.1021/acs.chemrev.6b00018
26. Prier, C. K., Rankic, D. A., & MacMillan, D. W. C. (2013). Visible light photoredox catalysis with transition metal complexes: Applications in organic synthesis. *Chemical Reviews, 113*, 5322–5363. https://doi.org/10.1021/cr300503r
27. Schultz, D. M., & Yoon, T. P. (2014). Solar synthesis: Prospects in visible light photocatalysis. *Science, 343*, 1239176. https://doi.org/10.1126/science.1239176
28. Xuan, J., & Xiao, W.-J. (2012). Visible-light photoredox catalysis. *Angewandte Chemie International Edition, 51*, 6828–6838. https://doi.org/10.1002/anie.201200223
29. Beatty, J. W., & Stephenson, C. R. J. (2015). Amine functionalization via oxidative photoredox catalysis: Methodology development and complex molecule synthesis. *Accounts of Chemical Research, 48*, 1474–1484. https://doi.org/10.1021/acs.accounts.5b00068
30. Nakajima, K., Miyake, Y., & Nishibayashi, Y. (2016). Synthetic utilization of α-aminoalkyl radicals and related species in visible light photoredox catalysis. *Accounts of Chemical Research, 49*, 1946–1956. https://doi.org/10.1021/acs.accounts.6b00251
31. Majek, M., & Jacobi von Wangelin, A. (2016). Mechanistic perspectives on organic photoredox catalysis for aromatic substitutions. *Accounts of Chemical Research, 49*, 2316–2327. https://doi.org/10.1021/acs.accounts.6b00293
32. Ghosh, I., Marzo, L., Das, A., Shaikh, R., & Koenig, B. (2016). Visible light mediated photoredox catalytic arylation reactions. *Accounts of Chemical Research, 49*, 1566–1577. https://doi.org/10.1021/acs.accounts.6b00229
33. Jin, Y., & Fu, H. (2017). Visible-light photoredox decarboxylative couplings. *Asian Journal of Organic Chemistry, 6*, 368–385. https://doi.org/10.1002/ajoc.201600513
34. Xuan, J., Zhang, Z.-G., & Xiao, W.-J. (2015). Visible-light-induced decarboxylative functionalization of carboxylic acids and their derivatives. *Angewandte Chemie International Edition, 54*, 15632–15641. https://doi.org/10.1002/anie.201505731
35. Ravelli, D., Protti, S., Fagnoni, M., & Albini, A. (2013). Visible light photocatalysis. A green choice? *Current Organic Chemistry, 17*, 2366–2373. https://doi.org/10.2174/13852728113179990051
36. Reckenthler, M., & Griesbeck, A. G. (2013). Photoredox catalysis for organic syntheses. *Advanced Synthesis and Catalysis, 355*, 2727–2744. https://doi.org/10.1002/adsc.201300751
37. Teply, F. (2011). Photoredox catalysis by $[Ru(bpy)_3]^{2+}$ to trigger transformations of organic molecules. Organic synthesis using visible-light photocatalysis and its 20th century roots. *Collection of Czechoslovak Chemical Communications, 76*, 859–917. https://doi.org/10.1135/cccc2011078
38. Ghosh, I., Ghosh, T., Bardagi, J. I., & König, B. (2014). Reduction of aryl halides by consecutive visible light-induced electron transfer processes. *Science, 346*, 725–728. https://doi.org/10.1126/science.1258232
39. Barham, J. P., & König, B. (2020). Synthetic photoelectrochemistry. *Angewandte Chemie International Edition, 59*, 11732–11747. https://doi.org/10.1002/anie.201913767
40. Garnes-Portolés, F., Greco, R., Oliver-Meseguer, J., Castellanos-Soriano, J., Jiménez, M. C., López-Haro, M., Hernández-Garrido, J. C., Boronat, M., Pérez-Ruiz, R., & Leyva-Pérez, A. (2021). Regioirregular and catalytic Mizoroki-Heck reactions. *Nature Catalysis, 4*(4), 293–303. https://doi.org/10.1038/s41929-021-00592-3
41. Glaser, F., Kerzig, C., & Wenger, O. S. (2021). Sensitization-initiated electron transfer via upconversion: Mechanism and photocatalytic applications. *Chemical Science, 12*, 9922–9933. https://doi.org/10.1039/D1SC02085D
42. Castellanos-Soriano, J., Herrera-Luna, J. C., Díaz Díaz, D., Jiménez, M. C., & Pérez-Ruiz, R. (2020). Recent applications of biphotonic processes in organic synthesis. *Organic Chemistry Frontiers, 7*, 1709–1716. https://doi.org/10.1039/D0QO00466A
43. Ravetz, B. D., Pun, A. B., Churchill, E. M., Congreve, D. N., Rovis, T., & Campos, L. M. (2019). Photoredox catalysis using infrared light via triplet fusion upconversion. *Nature, 565*, 343–346. https://doi.org/10.1038/s41586-018-0835-2

44. Tokunaga, A., Uriarte, L. M., Mutoh, K., Fron, E., Hofkens, J., Sliwa, M., & Abe, J. (2019). Photochromic reaction by red light via triplet fusion upconversion. *Journal of the American Chemical Society, 141*, 17744–17753. https://doi.org/10.1021/jacs.9b08219
45. López-Calixto, C. G., Liras, M., de la Peña O'Shea, V. A., & Pérez-Ruiz, R. (2018). Synchronized biphotonic process triggering C–C coupling catalytic reactions. *Applied Catalysis B, 237*, 18–23. https://doi.org/10.1016/j.apcatb.2018.05.062
46. Kerzig, C., & Wenger, O. S. (2018). Sensitized triplet-triplet annihilation upconversion in water and its application to photochemical transformations. *Chemical Science, 57*, 6670–6678. https://doi.org/10.1039/C8SC01829D
47. Majek, M., Faltermeier, U., Dick, B., Pérez-Ruiz, R., & Jacobi von Wangelin, A. (2015). Application of visible-to-UV photon upconversion to photoredox catalysis: The activation of aryl bromides. *Chemistry A European Journal, 21*, 15496–15501. https://doi.org/10.1002/chem.201502698
48. Haering, M., Pérez-Ruiz, R., Jacobi von Wangelin, A., & Diaz Diaz, D. (2015). Intragel photoreduction of aryl halides by green-to-blue upconversion under aerobic conditions. *Chemical Communications, 51*, 16848–16851. https://doi.org/10.1039/C5CC06917C
49. Ackermann, L. (2009). *Modern Arylation Methods*. Wiley-VCH Verlag GmbH & KGaA.
50. Kalay, E., Küçükkeçeci, H., Kilic, H., & Metin, Ö. (2020). Black Phosphorus as a metal-free, visible-light active heterogeneous photoredox catalyst for the direct c-h arylation of heteroarenes. *Chemical Communications, 56*, 5901–5904. https://doi.org/10.1039/D0CC01874K
51. Schemalzbauer, M., Ghosh, I., & König, B. (2019). Utilising excited state organic anions for photoredox catalysis: Activation of (hetero)aryl chlorides by visible light-absorbing 9-anthrolate anions. *Faraday Discussions, 215*, 364–378. https://doi.org/10.1039/C8FD00176F
52. Wang, L., Byun, J., Li, R., Huang, W., & Zhang, K. A. I. (2018). Molecular Design of donor-acceptor-type organic photocatalysts for metal-free aromatic C–C bond formations under visible light. *Advanced Synthesis and Catalysis, 360*, 4312–4318. https://doi.org/10.1002/adsc.201800950
53. Bu, M.-J., Lu, G.-P., Jiang, J., & Cai, C. (2018). Merging visible-light photoredox and micellar catalysis: Arylation reactions with anilines nitrosated in situ. *Catalysis Science & Technology, 8*, 3728–3732. https://doi.org/10.1039/C8CY01221K
54. Maity, P., Kundu, D., & Ranu, B. C. (2015). Visible-light-photocatalyzed metal-free C-H heteroarylation of heteroarenes at room temperature: A sustainable synthesis of biheteroaryls. *European Journal of Organic Chemistry, 2015*, 1727–1734. https://doi.org/10.1002/ejoc.201500006
55. Zhang, J., Chen, J., Zhang, X., & Lei, X. (2014). Total syntheses of menisporphine and daurioxoisoporphine C enabled by photoredox-catalyzed direct C–H arylation of isoquinoline with aryldiazonium salt. *Journal of Organic Chemistry, 79*, 10682–10688. https://doi.org/10.1021/jo5020432
56. Cheng, Y., Gu, X., & Li, P. (2013). Visible-light photoredox in homolytic aromatic substitution: Direct arylation of arenes with aryl halides. *Organic Letters, 15*, 2664–2667. https://doi.org/10.1021/ol400946k
57. Hari, D. P., Schroll, P., & Koenig, B. (2012). Metal-free, visible-light-mediated direct C–H arylation of heteroarenes with aryl diazonium salts. *Journal of the American Chemical Society, 134*, 2958–2961. https://doi.org/10.1021/ja212099r
58. Neumeier, M., Sampedro, D., Májek, M., de la Peña O'Shea, V. A., Jacobi von Wangelin, A., & Pérez-Ruiz, R. (2018). Dichromatic photo-catalytic substitutions of aryl halides with a small organic dye. *Chemistry A European Journal, 24*, 105–108. https://doi.org/10.1002/chem.201705326
59. Chatterjee, A., & König, B. (2019). Birch-type photoreduction of arenes and heteroarenes by sensitized electron transfer. *Angewdte Chemie International Edition, 58*, 14289–14294. https://doi.org/10.1002/anie.201905485
60. Pal, A. K., Li, C., Hanan, G. S., & Zysman-Colman, E. (2018). Blue-emissive cobalt(III) complexes and their use in the photocatalytic trifluoromethylation of polycyclic aromatic hydrocarbons. *Angewdte Chemie International Edition, 57*, 8027–8031. https://doi.org/10.1002/anie.201802532
61. Graham, M. A., Noonan, G., Cherryman, J. H., Douglas, J. J., Gonzalez, M., Jackson, L. V., Leslie, K., Liu, Z.-Q., McKinney, D., Munday, R. H., Parsons, C. D., Whittaker, D. T. E., Zhang, E.-X., & Zhang, J.-W. (2021). Development and proof of concept for a large-scale photoredox additive-free minisci reaction. *Organic Process Research & Development, 25*, 57–67. https://doi.org/10.1021/acs.oprd.0c00483
62. Brown, M., Aljarah, M., Asiki, H., Leung, L. M. H., Smithen, D. A., Miller, N., Nemeth, G., Davies, L., Niculescu-Duvaz, D., Zambon, A., & Springer, C. (2021). Toward the scale-up of a bicyclic homopiperazine via schmidt rearrangement and photochemical oxaziridine rearrangement in continuous-flow. *Organic Process Research and Development, 25*, 148–156. https://doi.org/10.1021/acs.oprd.6b00213
63. Lévesque, F., Di Maso, M. J., Narsimhan, K., Wismer, M. K., & Naber, J. R. (2020). Design of a kilogram scale, plug flow photoreactor enabled by high power LEDs. *Organic Process Research and Development, 24*, 2935–2940. https://doi.org/10.1021/acs.oprd.0c00373
64. Cambié, D., Bottecchia, C., Straathof, N. J. W., Hessel, V., & Noël, T. (2016). Applications of continuous-flow photochemistry in organic synthesis, material sciences, and water treatment. *Chemical Reviews, 116*, 10276–10341. https://doi.org/10.1021/acs.chemrev.5b00707